Canadian Mineralogist
Vol. 30, pp. 49-59 (1992)

THE ORIGIN OF THE SUPERSTRUCTURE AND MODULATIONS IN CANCRINITE

ISHMAEL HASSAN* AND PETER R. BUSECK
Departments of Geology and Chemistry, Arizona State University, Tempe, Arizona 85287, U.S.A.

ABSTRACT

High-resolution transmission electron microscopy (HRTEM) has been used to study the complex satellite reflections in a carbonate-rich hexagonal cancrinite, $Na_{6.0}Ca_{1.5}[Al_6Si_6O_{24}](CO_3)_{1.6}\bullet 1.8H_2O$, with an *a* of 12.590, and a *c* of 5.117 Å. These reflections indicate a supercell with the same *a* dimension as the substructure, but with a *c* dimension that is eight times that of the substructure ($8 \times c = 40.94$ Å). All seven rows of superstructure satellite reflections were observed. The superstructure can be explained by ordering of cations, anions, and vacancies that occur in the channels of cancrinite. HRTEM images show the positions of the CO_3-group vacancies and associated Ca-atom vacancies, *i.e.*, $[Ca\bullet CO_3]$ vacancies in the supercells. The ordering of $[Ca\bullet CO_3]$ clusters and their vacancies, and ordering of Na and Ca cations and Ca vacancies on the Na2 site, give rise to the superstructure in cancrinite. A superstructure model is presented in which the chemical composition, degree of nonstoichiometry, and formation of superstructures in cancrinite are rationalized in terms of available space and coordinations of the Na2 site in the channels.

Keywords: cancrinite, high-resolution transmission electron microscopy, crystal structure, superstructure, $[Ca\bullet CO_3]$ vacancy, order, modulated structure, sodalite, zeolite.

SOMMAIRE

Nous avons utilisé la microscopie électronique à transmission à haute résolution pour étudier les réflexions satellites complexes d'une cancrinite carbonatée hexagonale, $Na_{6.0}Ca_{1.5}[Al_6Si_6O_{24}](CO_3)_{1.6}\bullet 1.8H_2O$, dont les paramètres *a* et *c* sont 12.590 et 5.117 Å, respectivement. Ces réflexions sont la manifestation d'une surstructure dont la maille partage la même dimension *a* que la sous-structure, mais dont la périodicité *c* est huit fois celle de la sous-structure (40.94 Å). Chacune des sept rangées de réflexions satellites a été observée. Nous attribuons la surstructure à une mise en ordre des cations, anions, et lacunes dans les canaux de la structure. Les images à haute résolution montrent la position des lacunes impliquant les groupes de CO_3 ainsi que les lacunes associées impliquant le site du Ca, c'est-à-dire, les lacunes impliquant $[Ca\bullet CO_3]$ dans la surstructure. La mise en ordre des groupements $[Ca\bullet CO_3]$ et des lacunes impliquant ce groupement, ainsi que des cations Na et Ca et des lacunes impliquant le Ca sur le site Na2, est à l'origine de la surstructure dans la cancrinite. Nous proposons un modèle qui prédit la composition chimique, l'écart à la stoechiométrie, et la formation de surstructures dans la cancrinite à partir des sites disponibles et de la coordinence du site Na2 dans les canaux.

(Traduit par la Rédaction)

Mots-clés: cancrinite, microscopie électronique à transmission à haute résolution, structure cristalline, mise en ordre des lacunes $[Ca\bullet CO_3]$, modulation structurale, sodalite, zéolite.

INTRODUCTION

The cancrinite-group minerals are framework aluminosilicates that occur in silica-deficient, alkali-rich rocks. These minerals are of interest because they are rock-forming aluminosilicates, contain volatile elements, and share structural units with the industrially important zeolites. The cages in cancrinite are the same as the building units in many zeolites. The cancrinite-group minerals have complicated and rather interesting chemistries: they contain large anionic groups, and many are nonstoichiometric. Structurally, they are of special interest because they display intriguing satellite reflections that vary markedly with composition and temperature, thus giving rise to complex modulated superstructures.

The structures of the cancrinite-group minerals are characterized by a network of $(Al,Si)O_4$ tetrahedra in which the Al and Si cations are fully ordered. Their structures consist of parallel six-membered rings consisting of alternating AlO_4 and SiO_4 tetrahedra. The hexagonal symmetry, $P6_3$, is the result of the stacking of such six-membered rings in an *ABAB*... sequence. This stacking gives rise to large continuous channels parallel to the 6_3 axis (*z* axis); these channels are formed by twelve-membered rings of alternating AlO_4 and SiO_4 tetrahedra. The structure also consists of "chains" of small cages ["undecahedral" or α-cages that are bounded by six four-membered

*Present address: Department of Geology, University of Kuwait, P.O. Box 5969, Safat 13060, Kuwait.

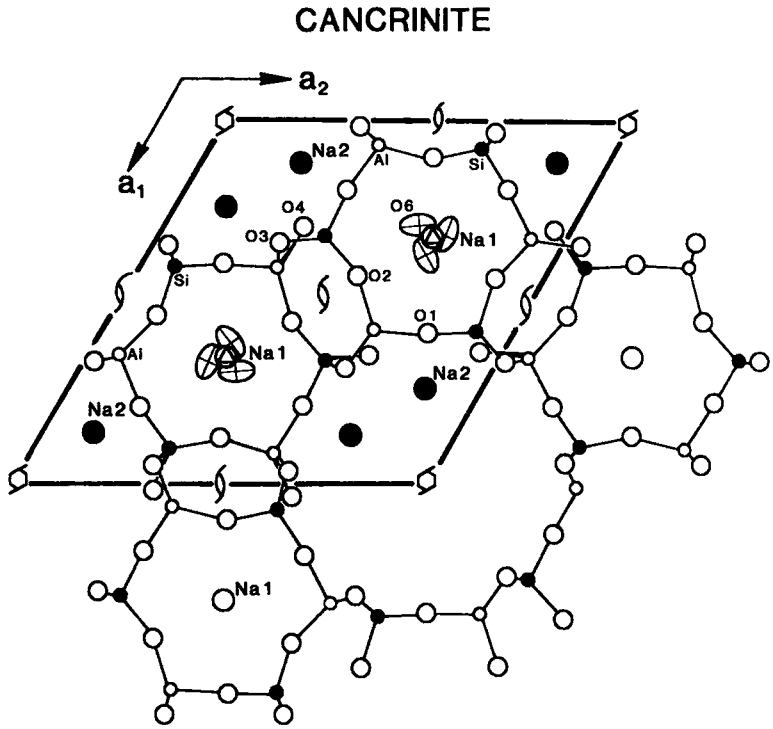

FIG. 1. Projection of the structure of cancrinite down [001] showing the site nomenclature, symmetry elements for space group $P6_3$, large channels along the 6_3 axes, and cages along the 3-fold axes (Papike 1988, modified from Grundy & Hassan 1982).

and five six-membered $(Al,Si)O_4$ rings] along the three-fold axes that are parallel to the z axis (Fig. 1).

Cancrinite-group minerals have strong structural similarities to the sodalite-group minerals. However, the latter have an *ABCABC...* stacking sequence of six-membered rings that leads to cubic instead of hexagonal symmetry. This sequence leads to an offset of the channels by the *C*-type layer and gives rise to a network of large cages in the sodalite-group minerals instead of continuous channels as in the cancrinite-group minerals.

The minerals of interest in this paper include vishnevite, basic (hydroxyl) cancrinite, davyne, and, in particular, cancrinite (Table 1). The ideal end-member formula for cancrinite is $Na_6Ca_2[Al_6Si_6O_{24}](CO_3)_2 \bullet 2H_2O$. However, many cancrinite-group minerals are nonstoichiometric, and the composition of the specimen used in the present study is $Na_{6.0}Ca_{1.5}[Al_6Si_6O_{24}](CO_3)_{1.6} \bullet 1.8H_2O$. The results obtained from this cancrinite can then be used to discuss the superstructures in other members of the cancrinite group.

Satellite reflections are commonly observed in

TABLE 1. COMPOSITIONS OF CANCRINITE-GROUP MINERALS AND INFORMATION ABOUT CAGE CLUSTERS

Minerals	Ideal Formulae	Cage clusters	Channel Ions	R	Reference
Cancrinite	$Na_6Ca_2[Al_6Si_6O_{24}](CO_3)_2 \cdot 2H_2O$	$[Na \cdot H_2O]^+$	Na, Ca, CO_3	0.028	Grundy & Hassan (1982)
Basic (hydroxyl) Cancrinite	$Na_8[Al_6Si_6O_{24}](OH)_2 \cdot 3H_2O$	$[Na \cdot H_2O]^+$	Na, OH, H_2O	0.047	Hassan & Grundy (1991a)
Vishnevite	$Na_8[Al_6Si_6O_{24}](SO_4) \cdot 2H_2O$	$[Na \cdot H_2O]^+$	Na, K, SO_4	0.037	Hassan & Grundy (1984)
Davyne	$Na_6Ca_2[Al_6Si_6O_{24}]Cl_2(OH)_2$	$[Ca \cdot Cl]^+$	Na, Ca, K, OH	0.048	Hassan & Grundy (1990)

cancrinite-group minerals (Jarchow 1965, Foit *et al.* 1973), but their origins are not known in detail. The satellite reflections indicate distinct supercells with various values for the *c* parameter (Brown & Cesbron 1973). Details of satellite reflections from cancrinite-group minerals differ for each mineral and differ among specimens from different localities. In addition to distinct chemistries, the satellite reflections are related to the temperature of formation of the minerals and the ordering processes associated with decreasing temperature.

Grundy & Hassan (1982) studied a carbonate-rich cancrinite (the same specimen as is used in the present study) with well-developed satellite reflections using X-ray-diffraction analysis, high-resolution transmission electron microscopy (HRTEM), and selected-area electron diffraction (SAED) analysis. They excluded the possibility that the satellite reflections arise from periodic variations in the stacking sequence of the six-membered rings. Their HRTEM image did not contain information on the satellite reflections because the order giving rise to such reflections is easily destroyed by the electron beam. Therefore, other features that may be periodic, such as stacking faults, antiphase domain boundaries, or twinning, could not be ruled out as the cause(s) of the satellite reflections.

Here we present new HRTEM data on the superstructure in cancrinite to determine its origin; the results support the superstructure model of Grundy & Hassan (1982). The present study indicates that the superstructure arises from ordering of the atoms and vacancies that occur in the channels of cancrinite. The present results show the positions of the CO_3-group vacancies in the supercells. Such vacancies are associated with Ca-atom vacancies. Three $[Ca{\bullet}CO_3]$ vacancies occur in a supercell.

Structure of Cancrinite-Group Minerals

The origins of the satellite reflections in the cancrinite-group minerals are not known. In the first phase of this project, the substructures of several cancrinite-group minerals thus were refined using single-crystal X-ray diffraction data; the pertinent crystal-chemical data are summarized in Table 1. One of the aims was to provide accurate structural data to form a basis for the development of superstructure models to explain the various satellite-reflections that occur in the cancrinite-group minerals. The average substructures include the effects of positional and compositional modulations, so that such substructures contain information about the superstructures. The X-ray structural data, therefore, form a useful starting point for an understanding of the superstructures of cancrinite-group minerals.

The cages in most cancrinite-group minerals contain one $[Na{\bullet}H_2O]^+$ cluster, although davyne contains $[Ca{\bullet}Cl]^+$ clusters. The Na atom is on the Na1 site, and the H_2O molecule is disordered around the three-fold axis because of hydrogen bonding (O6 oxygen in Fig. 1). In davyne, Ca rather than Na occurs on the Na1 site, and Cl occurs on the three-fold axis in place of H_2O. The framework atoms, $[Al_6Si_6O_{24}]$, and the atoms that form the cage clusters are not involved in the superstructures because these atoms show no unusual features in the X-ray structural models.

The atoms giving rise to the superstructures occur in the channels. The channels contain the remaining cations (Na^+, Ca^{2+}, and K^+ on the Na2 site), and anions (CO_3^{2-}, SO_4^{2-}, OH^- and H_2O), and vacancies commonly occur on these channel sites. The CO_3 and SO_4 groups in cancrinite and vishnevite, respectively, are disordered over two alternative positions unrelated by symmetry (each of multiplicity two) with equal probability. A triangular face of the SO_4 tetrahedron in vishnevite has an orientation similar to that of the triangular CO_3 group in cancrinite, with an apical oxygen atom of the SO_4 group pointing either up or down along the 6_3 axis. The OH and H_2O groups in the channels of basic (hydroxyl) cancrinite are in positions similar to those of the oxygen atoms of the CO_3 group in cancrinite.

In the average substructure of cancrinite, the C atom of the CO_3 group is at (0, 0, *z*). The C atoms occupy two split positions: C1 and C2, and C1′ and C2′. The *z* values for the C1 and C2 split positions are 0.6729 and 0.9137, respectively, and their symmetry-related split positions, C1′ and C2′, have *z* values of 0.1729 and 0.4137, respectively. All four C positions are statistically equally occupied; each has an occupancy factor of 0.38. The important distances between the C atom positions are: for C1–C2, 1.23 Å, for C1–C1′ and C2–C2′, 2.56 Å, for C1–C2′ and C1′–C2, 3.79 Å, and for C1–C2 and C1′–C2′, 3.88 Å. For some of these distances, the C atoms are located in adjacent subcells. However, the 1.23 A distance is too short to permit both positions to be occupied simultaneously in a unit subcell. These distances will be discussed further below. The four C positions and their deficient site-occupancies lead to the possibility of an ordering of the CO_3 groups and their vacancies in forming superstructures in cancrinite. This ordering is associated with consequent re-arrangement of cations and vacancies on the Na2 site.

Electron Microscopy

The specimen used in this study is from Dungannon Township, Ontario (McMaster University collection #68024). The chemical composition

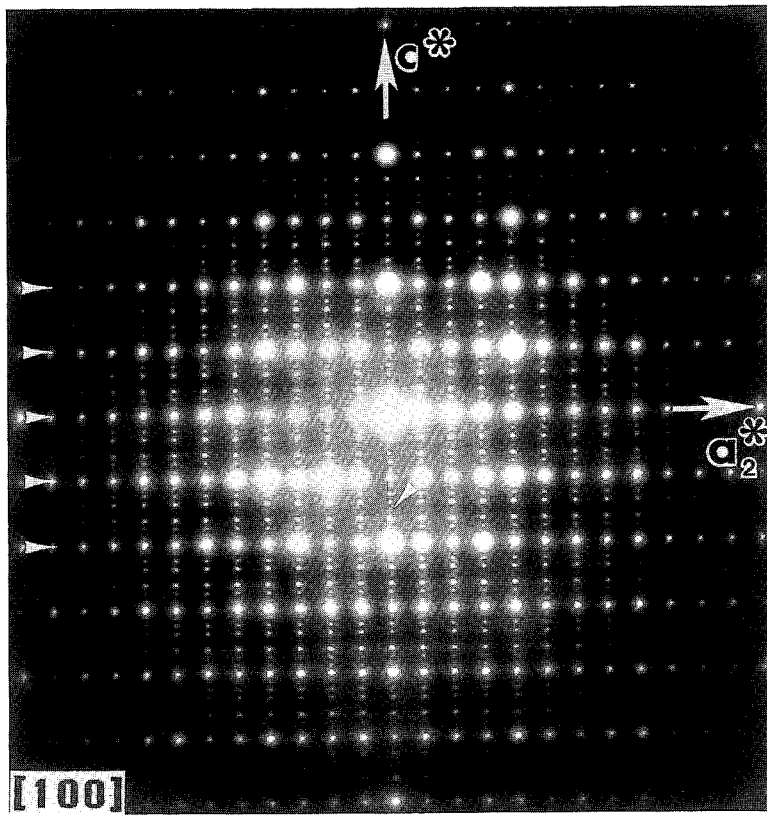

FIG. 2. [100]-zone SAED pattern of cancrinite containing strong rows of substructure reflections (arrows), with seven rows of weaker satellite reflections between adjacent substructure rows parallel to a^*_2 and giving rise to an 8 × c supercell.

is $Na_{5.96}Ca_{1.52}[Al_6Si_6O_{24}](CO_3)_{1.57}\bullet 1.75H_2O$, with hexagonal symmetry, cell parameters a 12.590, c 5.117 Å, and a supercell of 8 × c (= 40.936 Å; Grundy & Hassan 1982).

Fragments of cancrinite were obtained by crushing in acetone using an agate mortar and pestle. The fragments in suspension were deposited on holey carbon support films, and HRTEM data were recorded from thin regions. Electron microscopy was performed using a JEOL 4000EX microscope operated at 400 keV and equipped with a ±15° double-tilt, top-entry goniometer stage; C_s was 1.0 mm. HRTEM images were recorded using the minimum exposure mode.

The [100] zone SAED pattern is from a section of the crystal that is parallel to the (210) plane, and it contains the 6_3 axis (z axis; Fig. 2). There are seven rows of satellite reflections that are parallel to a^*_2 and occur between adjacent rows of substructure reflections (indicated by arrow at the left of the figure), thus giving rise to a supercell of 8 × c. Some rows of satellite reflections are prominent, whereas others are weak (central arrow). With X-ray diffraction, many rows of satellite reflections are unobservable (*e.g.*, precession photographs in Brown & Cesbron 1973, Grundy & Hassan 1982, Hassan & Grundy 1984). However, in long-exposure (2 to 3 months) photographs, all the satellite reflections are present (Hassan 1983), which excludes the possibility that the satellite reflections arise from multiple diffraction in the SAED pattern. The rows of satellite reflections are parallel to each other in the SAED pattern, so that the possibility of positional modulations of the structure may be excluded (Buseck & Cowley 1983, Hassan & Buseck 1989a, b). The SAED pattern shows 00l, l = odd substructure reflections that are forbidden in space group $P6_3$. These reflections were not observed in X-ray precession photographs and are attributed to either multiple diffraction or superposition of satellite reflections.

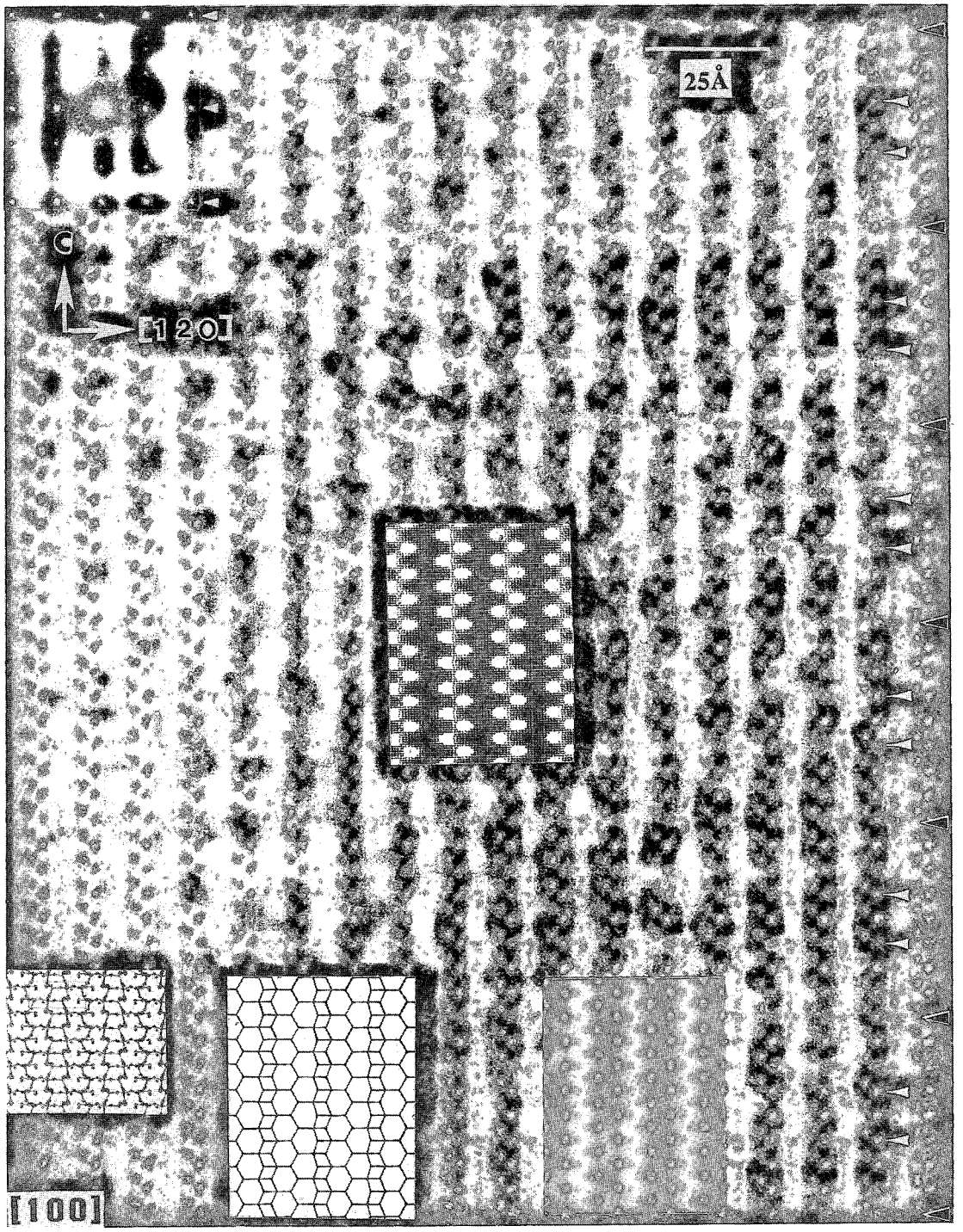

FIG. 3. HRTEM image down the [100] zone of cancrinite. The faint white lines (arrows at right) are superstructure fringes that are perpendicular to c. These white lines correspond to [Ca•CO_3] vacancies. The black arrowheads at the right indicate the supercell repeat. The top-left inset is an optical diffractogram in which the substructure rows of reflections are indicated by arrows, and the rows of satellite reflections occur between the arrows. Bottom insets are the projected structure (left), schematic diagram of the Al–Si framework (center), and an out-of-focus print of the schematic diagram (right). The central inset is the calculated image based on the average substructure.

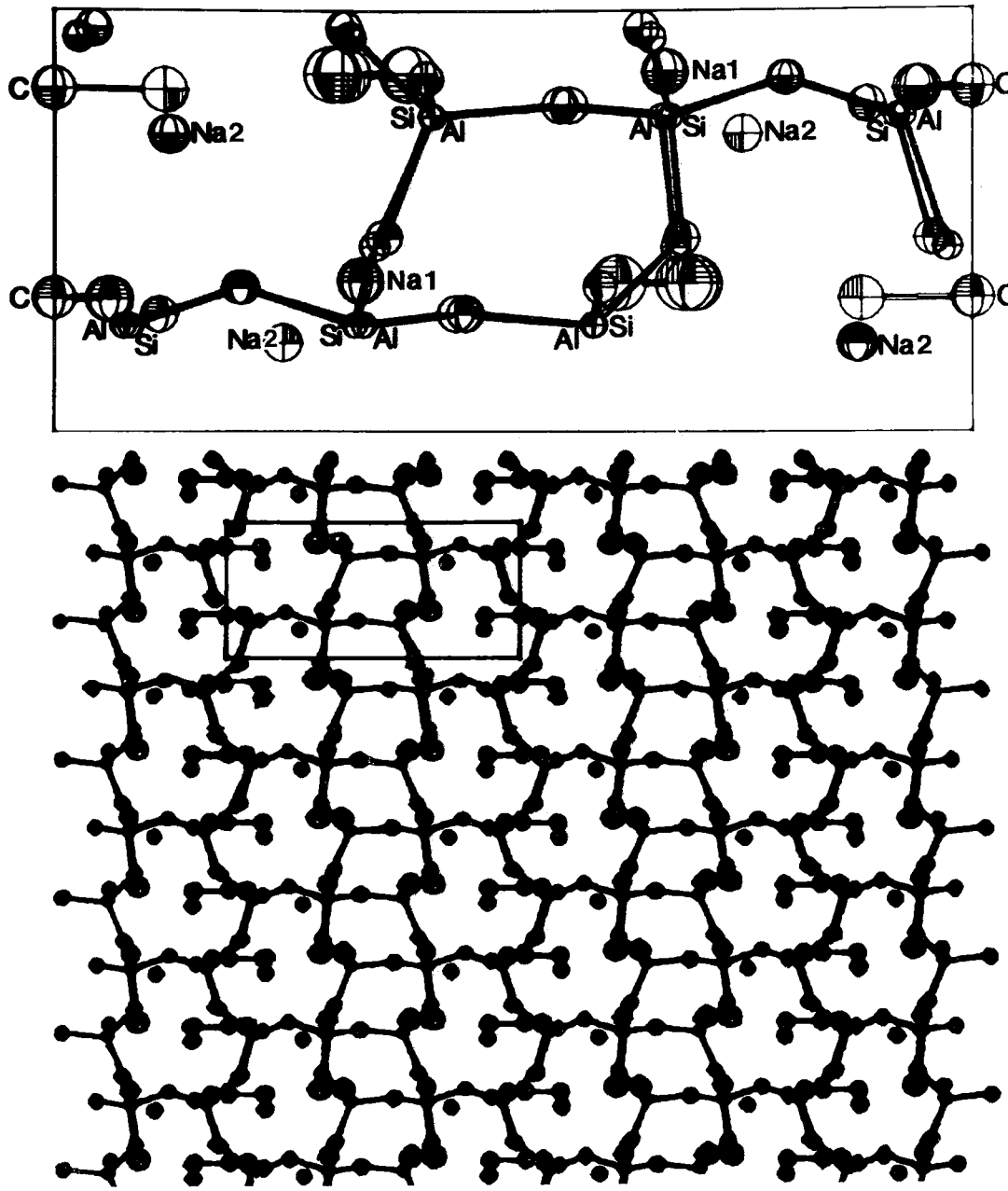

FIG. 4. Projections of the cancrinite structure down [100]: top: one unit subcell showing its content; only two of the four average C-atom positions are shown. Bottom: several unit subcells with one unit subcell outlined; the small edge is 5.117 Å in dimension.

The optical diffractogram of the HRTEM image (Fig. 3) contains rows of satellite reflections between rows of substructure reflections (indicated by arrow), so that the information regarding the satellite reflections is contained in the image that corresponds to the SAED pattern shown in Figure 2. The optical diffractogram is bounded by reflections of type 00 $\pm$ 1 and 0 $\pm$ 20, which are based on the subcell with c = 5.117 Å. The three rows of substructure reflections are pointed out by

arrows; the unmarked rows are the satellite reflections. The HRTEM image contains faint white lines that correspond to the superstructure fringes that are perpendicular to the *c* axis (arrows at right). The black arrowheads correspond to the period of the supercell repeat (40.94 Å). The white

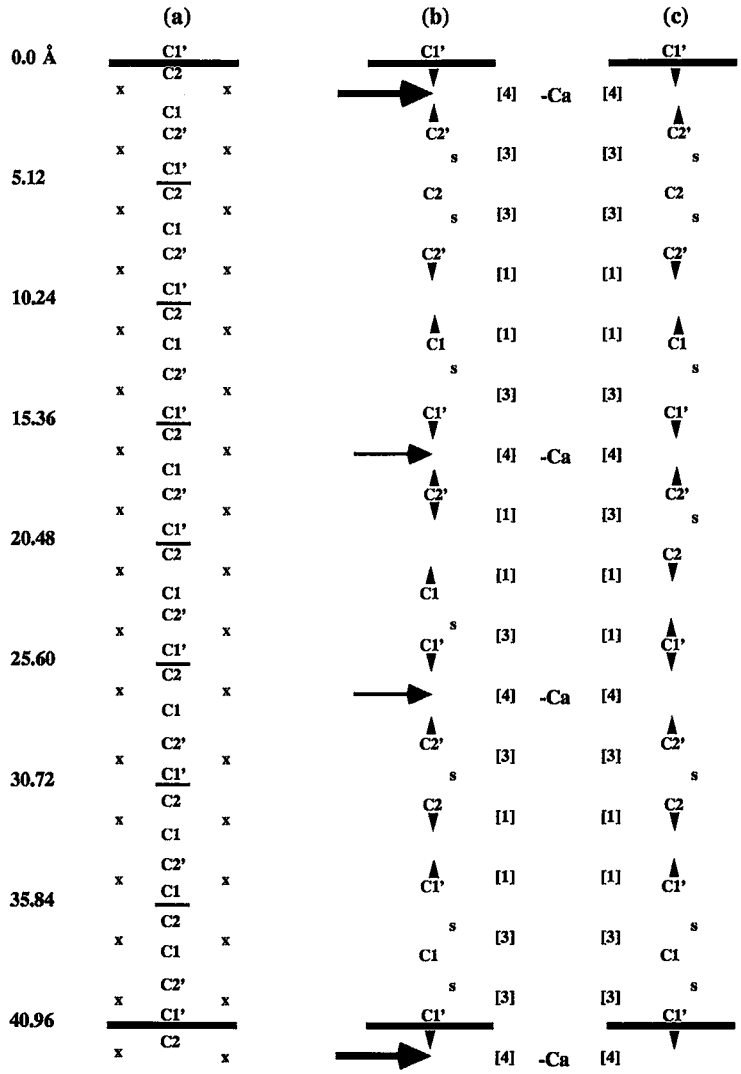

FIG. 5. (a) The average positions of the CO_3 groups (denoted by C1, C2, C1′, and C2′) and the Na2 positions (planes denoted by x) in a channel of a supercell in cancrinite. (b) and (c): Models of order of the ions and vacancies in a supercell. Filled Na2 positions are not shown in (b) and (c), but filled C positions are indicated. The four horizontal arrows point out vacancies in CO_3 groups and associated Ca atom; the latter are denoted by -Ca. The two large arrows point out a supercell repeat; they correspond to pairs of black arrows in Figure 3, whereas the pair of small arrows correspond to the pairs of white arrows in Figure 3. The letter s denotes C–C distance of 2.56 Å. The C–C distances of 3.79 or 3.88 Å are unlabeled. The vertical arrowheads indicate slight displacements of the CO_3 groups along the *z* axis. The numbers (1, 3, and 4) indicate the number of O atoms from the CO_3 groups coordinated to the Na2 site. The difference between the (b) and (c) models of order occurs in the region between the middle two horizontal arrows; elsewhere the models are identical.

arrowheads point out two additional faint white lines within each supercell. These white lines correspond to carbonate-group and associated Ca-atom omissions (see below); there are three such [Ca•CO_3] omissions within a supercell. The white lines are unevenly spaced (about 15 A away from either edge of a supercell; Figs. 3, 5).

The crystal structure projected down the [100] zone of cancrinite is shown as a bottom-left inset in Figure 3. An enlarged print of this projected structure, together with the unit-cell content, is given in Figure 4. The small rectangular box corresponds to one substructure cell; the short edge is approximately 5 Å in dimension (bottom of Fig. 4). A schematic diagram showing the *ABAB*... stacking sequence of the Al–Si framework is given as the central inset along the bottom of Figure 3 to emphasize the double set of six-membered rings in the projected structure. An out-of-focus print of this schematic diagram shows the six-membered rings as white dots that correspond to the white dots in the HRTEM image (bottom-right inset in Fig. 3)

Cancrinite is extremely unstable in the electron beam; it was thus not possible to obtain the usual through-focus series of images. Instead, interpretation of the HRTEM image was achieved through image calculations. Such images were calculated for the average substructure of cancrinite using the SHIRLI set of programs (O'Keefe & Buseck 1979, O'Keefe *et al.* 1978). Images were calculated for the [100] zone over a range of defocus values and thicknesses. Calculations were performed using the electron-optical parameters given above for the JEOL 4000EX microscope, together with a divergence angle of 0.8 milliradians, a depth of focus of 95 Å, and an objective aperture of 0.6 $Å^{-1}$.

A calculated image, based on the average structure of cancrinite, is given as the central inset in Figure 3. This image is based on a thickness of 76 Å and a defocus value of −500 Å. For these values, areas of light contrast correspond to regions of low density of electrons. The positions of the six-membered windows can be seen as white dots in the HRTEM image, and the additional faint white lines can be interpreted as CO_3 vacancies. Because such anion vacancies are associated with Ca-atom vacancies (for charge balance), the HRTEM image indicates both Ca and CO_3 vacancies, *i.e.*, [Ca•CO_3] vacancies (Fig. 5).

Differences between the calculated image for the average substructure and the present experimental HRTEM image can be attributed to the superstructure in cancrinite. The main difference between these two images is the presence of faint white lines in the HRTEM image, which is attributed to [Ca•CO_3] vacancies. Such vacancies are also indicated in the chemical composition and in the X-ray structural model, and their positions can be obtained from the HRTEM image.

Discussion

In the average substructure of cancrinite, the carbonate groups occur in the channels along the 6_3 axes, with their C atoms in two distinct positions (C1 and C2), 1.23 Å apart; each site has an occupancy of 0.38. The C atoms occur on two additional symmetry-related positions (C1′ and C2′). The Na2 site also is located in the channels, and in the average substructure, each Na2 position contains 0.67 Na, 0.25 Ca, and 0.08 vacancies. The occupancy of the C atom positions indicates three to four CO_3-group vacancies within the period of a supercell ($8 \times c = 40.94$ Å; Fig. 5). The superstructure in cancrinite is related to the ordering of such carbonate-group omissions, with consequent ordering of cations and their vacancies on the Na2 site (Grundy & Hassan 1982). From the great number of possibilities, a superstructure model was established through computer simulations of all possible combinations of ordering patterns. A good match was obtained between calculated and observed 00*l* satellite reflections, both in X-ray diffraction and SAED patterns (Grundy & Hassan 1982).

According to the chemical analysis, a channel in a supercell of cancrinite contains 31.68 Na, 12.12 Ca cations, and 12.56 CO_3 anions. The stoichiometric composition for a channel should be 48 (Na + Ca), *i.e.*, 32 Na and 16 Ca, and 16 CO_3 (32 half-occupied positions). This distribution gives rise to 3.44 CO_3-group vacancies and about 4.2 (Ca + Na) vacancies in a channel of a supercell. However, the HRTEM image indicates three carbonate-group omissions per supercell. Therefore, the superstructure is related to ordering of three CO_3-group vacancies, together with 32 Na, 13 Ca cations, and three Ca-atom vacancies (for charge balance) on the Na2 site in a channel of a supercell. The Na2 is a six-fold site; the cations occur in groups of three because of the 6_3 symmetry axis. In each group, the cations occur in a triangular configuration.

Results of the chemical analysis indicate a 1:1 correspondence between CO_3 and Ca; therefore, there are three vacant [Ca•CO_3] clusters and thirteen occupied [Ca•CO_3] clusters. Thus, a Ca atom is associated with each CO_3 group. The positions of the [Ca•CO_3] vacancies were located on the HRTEM image, and therefore the filled CO_3-group positions could be deduced. The Ca atoms and their vacancies can order on a spiral down the channels. In this ordering model, each subcell part of the channel contains a net charge of 4+ (corresponding to four Na cations), so that

the charge is evenly distributed along the channels. The ordering of the channel ions and their vacancies gives rise to the superstructure in cancrinite. A similar type of ordering model was computer-simulated by Grundy & Hassan (1982). However, in the present superstructure model, the number and positions of [Ca•CO_3] vacancies were observed in the HRTEM image. The present model is thus more advanced than that given by Grundy & Hassan (1982), where such vacancies were not directly observable. More importantly, both models indicate that only the ordering of the channel ions needs to be considered in rationalizing the superstructure in cancrinite-group minerals.

Two superstructure models are shown schematically in Figure 5. The C atom positions (C1, C2, C1′, and C2′) are indicated in the average substructure, and each cation plane that contains two Na and one Ca atom on the Na2 site is denoted by x (Fig. 5a). Cation planes that contain a vacant Ca atom are denoted by –Ca (Figs. 5b, c). The occupied C-atom positions are indicated in Figures 5b and c, and their displacements are indicated by vertical arrowheads. Of the two possible superstructure models, (b) has seven occupied C1 (and C1′) positions and six occupied C2 (and C2′) positions, and (c) has six occupied C1 positions and seven occupied C2 positions. Equal numbers of (b) and (c) ordering give rise to equal occupancy of C1 and C2, as indicated by the X-ray structure refinement. The (b) and (c) ordering can occur in different channels or in different parts of the same channel.

The superstructure models have seven long C–C distances (3.79 or 3.88 Å) and seven short distances (2.56 Å). The short distances are denoted by s, and the long distances are unlabeled (Figs. 5b, c). The long and short distances are distributed throughout the supercells. Such distribution of the CO_3 groups releases structural strain.

If only C–C distances of 2.56 Å occur, a cancrinite containing two CO_3 groups per unit subcell is possible, and this will give rise to the ideal end-member formula for cancrinite (Table 1). However, such a fully occupied CO_3-rich cancrinite cannot contain a superstructure and may be unstable because of large structural strains. Specimens of carbonate cancrinite contain superstructures. Therefore, a few long C–C distances are required to stabilize cancrinite, and this naturally leads to samples of CO_3-deficient cancrinite that display different superstructures.

If only long C–C distances occur, and the average CO_3 content from eight subcells is calculated, cancrinite would contain 1.250 or 1.357 CO_3 groups per unit subcell, compared to 1.63 CO_3 in the present specimen. However, cancrinite contains a maximum of about 1.7 CO_3 groups. Therefore, the structure of cancrinite can accommodate both C–C distances of 2.56 and 3.8 Å. Presumably, there is a limit to the number of 2.56-Å C–C distances that can occur in the structure.

Furthermore, the 2.56-Å C–C distance can be increased by slight displacements of the CO_3-groups along the z axis, as indicated by the vertical arrowheads (Figs. 5b, c). The elongation of the thermal ellipsoids for the CO_3-group atoms parallel to the z axis indicates that such displacements do occur (Grundy & Hassan 1982). The average of the thirteen C–C distances within a supercell is 3.15 Å, which is a reasonable distance. This result indicates that CO_3-group displacements are favorable in cancrinite. These geometrical possibilities and [Ca•CO_3] vacancies allow for the formation of different superstructures in different samples of cancrinite.

The ordering of the channel ions that gives rise to the superstructure in cancrinite can be rationalized further by considering the coordinations of the Na2 site. There are two equally plausible coordinations for the Na2 site in the average substructure (see Fig. 7 in Grundy & Hassan 1982). In the average substructure, the Na2 site is six-coordinated; it is bonded to three framework O atoms and to three O atoms from the CO_3 groups. If the C1 positions are occupied, the Na2 site bonds to two O atoms of the CO_3 group that is above and to one such O atom from below in a trigonal bipyramidal coordination. If the C2 positions are occupied, however, the Na2 site bonds to one O atom from the CO_3 group that is above and to two such O atoms from below in an octahedral coordination. Bond-valence calculations about the Na2 site indicate that the two possible coordinations of the Na2 site are electrostatically equivalent. The Na2 site contains no marked anisotropy, which indicates that the framework is insensitive to the type of cation or vacancy on this site. Chemical variation and ordering on the Na2 site are accommodated solely by the positioning of the CO_3 groups within the channel.

In the superstructure models, the number of O atoms from the CO_3 groups coordinating the Na2 site is indicated (Figs. 5b, c). The number is 1, 3, or 4. The implications for each of these coordinations are as follows: (a) If three such bonds occur, the coordination of the Na2 site would be similar to that in the average substructure (see above), but the C–C distance would be short (2.56 Å). The mineral would thus be under structural strain. The release of the structural strain is accomplished by small displacements of the CO_3 groups along the z axis, positioning of their vacancies, and by variations in the coordination of the Na2 site to O atoms of the CO_3 groups. (b) If one such bond occurs, the CO_3 group is pulled along the z axis

toward the Na2 site. (c) If four such bonds occur, a [Ca•CO_3] vacancy is present. In this case, the associated plane of cations contains two Na atoms, and the CO_3 groups are free to move either up or down along the *z* axis, depending on the positions of the neighboring C atoms. Because the neighboring positions have short C–C distances, the CO_3 groups move toward each other to take up the space left by a [Ca•CO_3] vacancy.

In both superstructure models (b) and (c), the displacement of one CO_3 group (indicated by double arrows) may be either up or down. This rationalization of the superstructure models indicates the close chemical communication between the various atoms and the vacancies: the framework regulates the Na2 site, which in turn influences the positions and vacancies of the CO_3 groups in the supercell. This effect also accounts for the chemical composition and the nonstoichiometry in cancrinite. In support and extension of the present structural model, the general nature of the superstructures in two other members of the cancrinite group is briefly discussed below.

The observed superstructure in vishnevite is attributed to ordering of the SO_4 group (Hassan & Grundy 1984). A unit subcell in vishnevite contains two symmetry-unrelated orientations of the SO_4 group (apical oxygen atom pointing either up or down). Equal occurrences of each SO_4 orientation would give a random pattern and no superstructure. However, if some correlation exists between channels, any up–down residual ordering of the SO_4 groups would give rise to superstructure formation. The ordering of the SO_4 groups together with a sympathetic ordering of the cations (Na, K, and Ca) on the Na2 site within the channels give rise to the observed satellite reflections in vishnevite. The superstructure features a doubling of the *c* axis.

Basic (hydroxyl) cancrinite is stoichiometric with respect to the interframework Na cations; in particular, the Na2 site is fully occupied by Na atoms (Hassan & Grundy 1991a). Therefore, the Na atoms on the Na2 site do not contribute to the satellite reflections, which arise from ordering of the OH and H_2O groups in the channels. The OH and H_2O groups in basic cancrinite are located in positions similar to those of the oxygen atoms of the CO_3 group in cancrinite. The superstructure features a tripling of the *c* axis.

The ordering of atomic species, as in cancrinite, is commonly called substitutional, atomic, or density ordering. The structures of cancrinite-group minerals can be modulated because the satellite reflections move with temperature and composition, so that the satellite reflections indicate density modulations. In suitable cases, density modulations can be distinguished from positional modulations using SAED patterns (Buseck & Cowley 1983); cancrinite- and sodalite-group minerals provide ideal examples of these types of modulations (Hassan & Buseck 1989a, b, Hassan & Grundy 1989, 1991b).

Conclusions

Many cancrinite crystals display extensive satellite reflections. These reflections can be rationalized as the effects of cation and anion ordering on atom sites that are located in the channels of cancrinite; such sites are positionally defined by the space group $P6_3$. An ordered arrangement of Ca, Na, and CO_3 ions, and [Ca•CO_3] vacancies over the available sites in the channels, according to the results of the chemical analysis, structure refinement, HRTEM imaging, and image calculations, has been established. The ordering of these atomic species gives rise to the satellite reflections in cancrinite. The HRTEM image of cancrinite shows the ordering of [Ca•CO_3] vacancies. Finally, the principles derived from cancrinite can be extended to other related cancrinite-like minerals, sodalite-group minerals, and zeolites.

Acknowledgements

We thank Dr. John Barry for help in using the 4000EX microscope, and Drs. H. Douglas Grundy and I. David Brown for their comments on this manuscript. Dr. J. David Embury provided support and encouragement, and we thank the referees Drs. S. Merlino and P. J. Heaney for useful reviews. The work was supported by NSF grant EAR-8708529, and the microscopy was done at the ASU HREM facility, which is supported by NSF and ASU.

References

Brown, W.L. & Cesbron, F. (1973): Sur les surstructures des cancrinites. *C.R. Acad. Sci. Paris* **276**(D), 1-4.

Buseck, P.R. & Cowley, J.M. (1983): Modulated and intergrowth structures in minerals and electron microscope methods for their study. *Am. Mineral.* **68**, 18-40.

Foit, F.F., Jr., Peacor, D.R. & Heinrich, E.W. (1973): Cancrinite with a new superstructure from Bancroft, Ontario. *Can. Mineral.* **11**, 940-951.

Grundy, H.D. & Hassan, I. (1982): The crystal structure of a carbonate-rich cancrinite. *Can. Mineral.* **20**, 239-251.

Hassan, I. (1983): *The Crystal Chemistry and Crystal*

Structures of the Sodalite and Cancrinite Groups of Minerals. Ph.D. thesis, McMaster Univ., Hamilton, Ontario.

_____ & BUSECK, P.R. (1989a): Incommensurate-modulated structure of nosean, a sodalite-group mineral. *Am. Mineral.* **74**, 394-410.

_____ & _____ (1989b): Cluster ordering and antiphase domain boundaries in hauyne. *Can. Mineral.* **27**, 173-180.

_____ & GRUNDY, H.D. (1984): The character of the cancrinite–vishnevite solid-solution series. *Can. Mineral.* **22**, 333-340.

_____ & _____ (1989): The structure of nosean, ideally $Na_8[Al_6Si_6O_{24}]SO_4 \bullet H_2O$. *Can. Mineral.* **27**, 165-172.

_____ & _____ (1990): Structure of davyne and implications for stacking faults. *Can. Mineral.* **28**, 341-349.

_____ & _____ (1991a): The crystal structure of basic cancrinite, ideally $Na_8[Al_6Si_6O_{24}](OH)_2 \bullet 3H_2O$. *Can. Mineral.* **29**, 377-383.

_____ & _____ (1991b): The crystal structure of hauyne at 293 and 153 K. *Can. Mineral.* **29**, 123-130.

JARCHOW, O. (1965): Atomanordnung und Strukturverfeinerung von Cancrinit. *Z. Kristallogr.* **122**, 407-422.

O'KEEFE, M.A. & BUSECK, P.R. (1979): Computation of high resolution TEM images of minerals. *Am. Crystallogr. Assoc. Trans.* **15**, 27-44.

_____, _____ & IIJIMA, S. (1978): Computed crystal structure images for high resolution electron microscopy. *Nature* **274**, 322-324.

PAPIKE, J.J. (1988): Chemistry of rock-forming silicates: multiple-chain, sheet, and framework structures. *Rev. Geophys.* **26**, 407-444.

Received July 14, 1990, revised manuscript accepted May 21, 1991.